Simultaneous measurement of thermal diffusivity and effusivity of solids using the flash technique in the front-face configuration

2015 Meas. Sci. Technol. 26 085017

(http://iopscience.iop.org/0957-0233/26/8/085017)

IOP Publishing Measurement Science and Technology
Meas. Sci. Technol. **26** (2015) 085017 (7pp) doi:10.1088/0957-0233/26/8/085017

Simultaneous measurement of thermal diffusivity and effusivity of solids using the flash technique in the front-face configuration

Nelson Wilbur Pech-May[1,2], Ángel Cifuentes[1,3], Arantza Mendioroz[1], Alberto Oleaga[1], and Agustín Salazar[1]

[1] Departamento de Física Aplicada I, Escuela Técnica Superior de Ingeniería, Universidad del País Vasco UPV/EHU, Alameda Urquijo s/n, 48013 Bilbao, Spain
[2] Department of Applied Physics, CINVESTAV Unidad Mérida, carretera Antigua a Progreso km6, A.P. 73 Cordemex, Mérida Yucatán 97310, Mexico
[3] Instituto Politécnico Nacional, CICATA Legaria, Av. Legaria No. 694 Col. Irrigación, 11500 Mexico D.F., Mexico

E-mail: agustin.salazar@ehu.es

Received 31 March 2015, revised 26 May 2015
Accepted for publication 28 May 2015
Published 16 July 2015

Abstract

Both thermal diffusivity and effusivity (or conductivity) are necessary to characterize the thermal transport properties of a material. The flash method is the most recognized procedure to measure the thermal diffusivity of free-standing opaque plates. However, it fails to simultaneously obtain the thermal effusivity (or conductivity). This is due to the difficulty of knowing the total energy absorbed by the sample surface after the light pulse. In this work, we propose using the flash method in the front-face configuration on a two-layer system made of the unknown plate and a fluid of known thermal properties. We demonstrate that the surface temperature is sensitive to the thermal mismatch between the plate and the fluid, which is governed by their thermal effusivity ratio. In order to verify the validity of the method and to establish its application limits we have performed flash measurements, using a pulsed laser and an infrared camera, on a set of calibrated materials (metals, alloys, ceramics and polymers) covering a wide range of thermal transport properties. These results confirm the ability of the flash method to simultaneously retrieve thermal diffusivity and effusivity in a fast manner in samples whose effusivities are lower than three times the effusivity of the liquid used as backing fluid.

Keywords: thermal diffusivity, thermal effusivity, flash method, infrared thermography

(Some figures may appear in colour only in the online journal)

1. Introduction

Characterizing the thermal transport properties of a material requires knowledge of two independent parameters: thermal diffusivity (D) and thermal effusivity (e) [1, 2]. Both are related to the more often acknowledged thermal conductivity (K) through the following relationship: $e = K/\sqrt{D}$. While steady-state methods are used to measure thermal conductivity, transient methods are sensitive to the couple D and e. In particular, the flash method has become a standard means to measure thermal diffusivity. It consists of heating the front face of an opaque plate by a brief light pulse and analysing the temperature evolution either at its rear surface, i.e. the classical configuration introduced by Parker *et al* more than fifty years ago [3], or at the illuminated surface, which is particularly useful for non-destructive testing

of materials since it only requires access to the free surface of the sample [4].

However, the flash method applied to free-standing plates only provides the thermal diffusivity. The reason for this can be understood by analysing the temperature history of the surfaces of an opaque plate of thickness L after being excited by an infinitely brief laser pulse under adiabatic conditions [5]

$$T(0) = \frac{Q_o\chi}{e}\frac{\sqrt{D}}{L}\left[1 + 2\sum_{n=1}^{\infty}\exp\left(-\frac{n^2\pi^2}{L^2}Dt\right)\right], \quad (1)$$

$$T(L) = \frac{Q_o\chi}{e}\frac{\sqrt{D}}{L}\left[1 + 2\sum_{n=1}^{\infty}(-1)^n\exp\left(-\frac{n^2\pi^2}{L^2}Dt\right)\right], \quad (2)$$

where Q_o is the energy per unit area delivered by the pulse, χ is the energy fraction absorbed by the sample, and $T(0)$ and $T(L)$ stand for the temperature at the illuminated and non-illuminated surfaces, respectively. As can be observed, the surface temperature depends on both D and e. However, they are correlated with other experimental magnitudes, Q_o and L. This means that only $Q_o\chi/e$ and $\sqrt{D}/L$ can be obtained. As the thickness of the sample can be easily measured, the flash method allows retrieval of the thermal diffusivity of the plate. However, the energy fraction absorbed by the sample surface is difficult to determine and therefore the thermal effusivity cannot be obtained accurately. This issue was already pointed out in the pioneering work on the flash method [3] (note that these authors referred to specific heat instead of thermal effusivity, since the multiplying factor in equations (1) and (2) can be rewritten as $\frac{Q_o\chi}{\rho cL}$, where ρ is the density and c the specific heat). Since then, several works have been published on retrieving the specific heat using the flash method, but they require an independent measurement of the laser pulse intensity and the reflectivity of the sample at the laser wavelength [6–9].

To overcome the above-mentioned drawback, putting the rear surface of the plate in contact with a fluid backing has been proposed [10, 11]. In this way, the front surface temperature will be sensitive to the thermal mismatch between plate and fluid, which is governed by the ratio of their effusivities. These studies were performed using modulated illumination, registering the amplitude and phase of the surface temperature as a function of the modulation frequency. Moreover, for normalization purposes (i.e. to eliminate the instrumental frequency dependence) the same frequency scan must be performed twice: with the sample backed by water and with the bare sample. Consequently, this procedure is rather time consuming (around 1 h).

Following the idea of using a fluid for thermal effusivity contrast, we propose in this work using the flash method in the front configuration to obtain D and e simultaneously in a fast manner. We have first calculated the front surface temperature of an opaque plate in contact with a fluid after being illuminated by a brief light pulse. The effect of the finite duration of the laser pulse as well as the heat losses by convection and radiation are also included in the model. By studying the sensitivity of the front surface temperature to D and e we show that both quantities are uncorrelated. Then, in order to establish the range of validity of the method we have performed experiments, using a pulsed laser and an infrared (IR) camera, on several calibrated materials (metals, alloys, ceramics and polymers) covering a wide range of thermal transport properties. These experiments show that the thermal effusivity of a sample can be retrieved accurately, provided it is smaller than three times the thermal effusivity of the liquid used as reference.

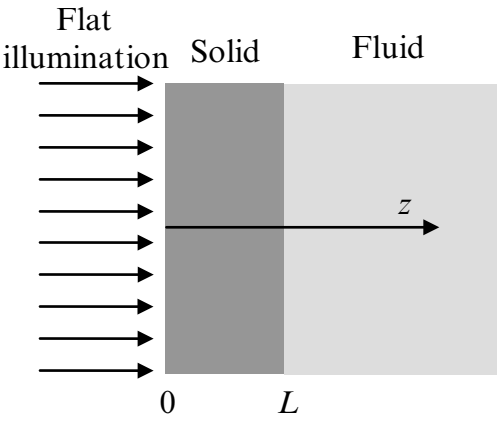

Figure 1. Diagram of the two-layer system made of an opaque solid slab and semi-infinite liquid backing. The front surface ($z = 0$) is uniformly illuminated by a brief laser pulse.

2. Theory

Let us consider a two-layer system made of an opaque solid slab of thickness L and a semi-infinite fluid backing. The free surface of the plate is illuminated uniformly by a brief laser pulse. The geometry of the problem is shown in figure 1. The Laplace transform of the temperature rise above the ambient in each medium is

$$\overline{T}_s(z) = Ae^{q_s z} + Be^{-q_s z} \quad (3a)$$

$$\overline{T}_f(z) = Ce^{-q_f(z-L)}, \quad (3b)$$

where $\overline{T}$ is the Laplace transform of the temperature, $q = \sqrt{s/D}$, being s the Laplace variable. Subscripts s and f stand for solid and fluid, respectively. Constants A, B and C are obtained from the boundary conditions at the interfaces

$$K_s\frac{d\overline{T}_s}{dz}\bigg|_{z=0} = h\overline{T}_s(z=0) - \overline{P}_o\chi, \quad (4a)$$

$$\overline{T}_s(z=L) = \overline{T}_f(z=L), \quad (4b)$$

$$K_s\frac{d\overline{T}_s}{dz}\bigg|_{z=L} = K_f\frac{d\overline{T}_f}{dz}\bigg|_{z=L}, \quad (4c)$$

where $\overline{P}_o$ is the Laplace transform of the temporal shape of the light beam and h is the linear coefficient of heat transfer, which takes into account the combined effect of heat convection and radiation. Note that heat transfer by convection at the solid–fluid interface has been neglected since its temperature

rise is small. The resulting expression for the Laplace transform of the temperature at the solid surface ($z = 0$) is

$$\overline{T}_s(0) = \frac{\overline{P}_o \chi}{e_s\sqrt{s}} \frac{\cosh(q_s L) + \frac{e_f}{e_s}\sinh(q_s L)}{\left(\frac{e_f}{e_s} + \frac{h}{e_s\sqrt{s}}\right)\cosh(q_s L) + \left(1 + \frac{h}{e_s\sqrt{s}}\frac{e_f}{e_s}\right)\sinh(q_s L)}. \quad (5)$$

In the following, we will consider two temporal shapes for the light pulse: (a) a delta function pulse and (b) a laser pulse. In the first case, the power distribution is $P_o(t) = Q_o\delta(t)$ and its Laplace transform is $\overline{P}_o = Q_o$, where Q_o is the energy per unit area delivered by the pulse and $\delta(t)$ is the Dirac delta function. The power distribution of a laser pulse follows an exponential law of the form $P_o(t) = \frac{Q_o}{N}\frac{t^\alpha}{\tau^{1+\alpha}}e^{-t/\tau}$, where α and τ are parameters which depend on the laser and N is a normalization constant in order to satisfy the condition $\int P(t)\,dt = Q_o$. Its Laplace transform is $\overline{P}_o = \frac{Q_o}{(1+s\tau)^{1+\alpha}}$. The power distribution of our laser pulse fits the exponential law with $\alpha = 1.46$ and $\tau = 0.132$ ms (see figure 2 in [12]).

By applying the inverse Laplace transform to equation (5), the time evolution of the surface temperature above the ambient after absorbing a laser pulse is obtained. To achieve this, the Stehfest algorithm [13] has been used, which gives very accurate results for 'smooth' functions [14], as in the case of $\overline{T}_s(0)$.

It is worth noting that equation (5) has been written in such a way that the degeneracy between parameters is clearly seen. Accordingly, $\overline{T}_s(0)$ depends on four fitting parameters: $Q_o\chi/e_s$, h/e_s, $L/\sqrt{D_s}$ and e_f/e_s. Therefore, a fitting of the time evolution of the front surface of an opaque slab on top of a fluid backing allows simultaneous retrieval of D_s and e_s, provided the thickness of the slab and the effusivity of the fluid are known.

3. Simulations

Numerical simulations showing the time evolution of the surface temperature $T_s(0)$ of an opaque solid slab with a water backing ($e_f = 1580\,\mathrm{W\,s^{0.5}\,m^{-2}\,K^{-1}}$) illuminated by a brief laser pulse are presented in figure 2. Ideal conditions are considered: a Dirac pulse ($\tau = 0$) and absence of heat losses ($h = 0$). Different values of the thermal effusivity of the solid slab, higher and lower than the effusivity of water, are analysed. In order to better compare the results, a normalized energy for the laser pulse is used in the simulations ($Q_o\chi/e_s = 1$). Moreover, by introducing the dimensionless time t/t_c, with $t_c = L^2/D_s$, we obtain a normalized temperature $T_s(0)$ which is independent of D_s and L values. As a reference, a simulation for an air backing ($e_{air} = 5.5\,\mathrm{W\,s^{0.5}\,m^{-2}\,K^{-1}}$) is also included.

As can be seen, at short times after the laser pulse, heat does not reach the rear surface of the solid and therefore the same straight line with slope −0.5 is obtained, independently of the thermal effusivities of sample and backing. At longer times, $T_s(0)$ becomes sensitive to the interface between sample and backing. When the backing is air, a horizontal straight line at long times is obtained. In fact, the intersection of both straight lines arises at $t_1 = L^2/(\pi D_s)$, which is used for thermal

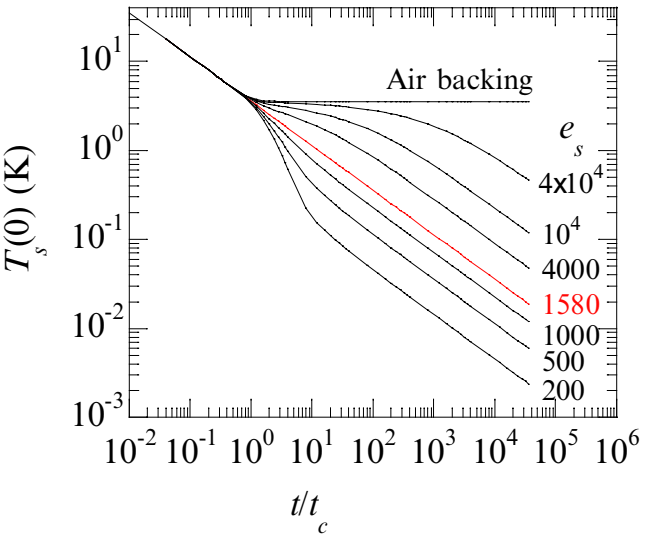

Figure 2. Simulation of the surface temperature evolution as a function of dimensionless time for an opaque slab on top of water ($e_f = 1580\,\mathrm{W\,s^{0.5}\,m^{-2}\,K^{-1}}$) after receiving a brief laser pulse ($Q_o\chi/e_s = 1$). Ideal conditions are considered: $h = \tau = 0$. Different values of the solid effusivity are evaluated. A simulation for air backing ($e_f = 5.5\,\mathrm{W\,s^{0.5}\,m^{-2}\,K^{-1}}$) is also plotted for comparison.

diffusivity identification [3]. It is worth noting that when the backing is air there is no sensitivity to the thermal effusivity of the sample. When the backing is water the behaviour of $T_s(0)$ at very long times is also a straight line of slope −0.5, but the position of this straight line varies depending on the thermal effusivity of the sample. If $e_s = e_f$ there is perfect thermal coupling between solid and fluid and accordingly a unique straight line is obtained at any time. If $e_s > e_f$ heat barely crosses the interface at $z = L$ and thermal energy is accumulated inside the solid slab. This explains why the temperature is above the straight −0.5 slope line for $t > t_1$. On the other hand, when $e_s < e_f$ heat easily crosses the interface and therefore there is a downwards displacement in temperature for $t > t_1$. From a practical point of view, the presence of water in contact with the solid slab allows us to obtain D_s and e_s simultaneously.

Now we analyse the sensitivity of the normalized $T_s(0)$ to both parameters in order to quantify the ability of the front-face flash method to retrieve them. Sensitivity of $T_s(0)$ to a given quantity x is defined as

$$Sy(x) = \frac{x}{T_s(0)}\frac{\partial T_s(0)}{\partial x}, \qquad \text{with } x = D_s \text{ or } e_s. \quad (6)$$

This equation does not have an analytical solution so numerical methods have been applied. The sensitivities of $T_s(0)$ to D_s and e_s are shown in figure 3. Numerical simulations have been performed for ideal conditions ($\tau = h = 0$). $Sy(D_s)$ is maximum for air backing, but the price to be paid is the lack of any information on e_s. The use of water as backing produces sensitivity to e_s, at the price of reducing $Sy(D_s)$. It is worth noting that the two sensitivities are not correlated: the highest $Sy(D_s)$ is produced at $t \approx 3.5t_c$, while the highest $Sy(e_s)$ appears at $t > 20t_c$. From figure 3(a) we can see that $Sy(D_s)$ is very small for samples with $e_s \approx e_f$, while it increases as e_s differs from e_f. This is related to the fact that the elbow in

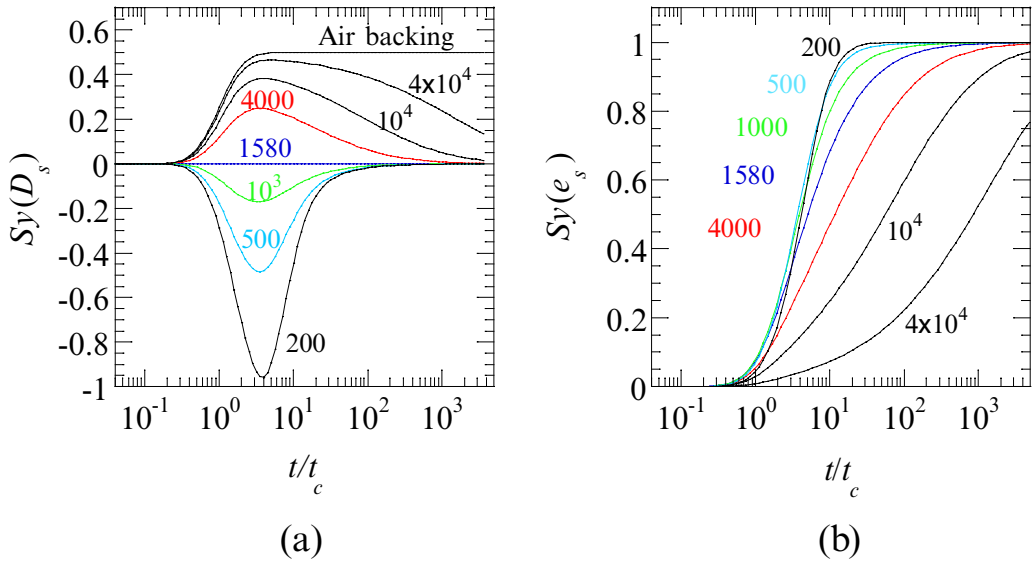

Figure 3. Sensitivity to (a) D_s and (b) e_s as a function of dimensionless time for an opaque slab on top of water ($e_f = 1580\,W\,s^{0.5}\,m^{-2}\,K^{-1}$) after receiving a brief laser pulse ($Q_\alpha\chi/e_s = 1$). Ideal conditions are considered: $h = \tau = 0$. Different values of the solid effusivity are evaluated. Sensitivity to D_s for air backing ($e_f = 5.5\,W\,s^{0.5}\,m^{-2}\,K^{-1}$) is also included for comparison.

$T_s(0)$ corresponding to the change in slope in figure 2 is barely noticeable for $e_s \approx e_f$, but becomes more pronounced as e_s and e_f values separate from each other. In fact, for samples with very low thermal effusivity, $Sy(D_s)$ is even higher using water backing than for air backing, e.g. for $e_s = 200$, $Sy(D_s) \approx -1$. In any case, note that for these materials the surface temperature at times corresponding to the highest $Sy(D_s)$, i.e. $t \approx 3.5t_c$, is very low and therefore affected by the experimental noise (in our experimental setup it is about 10 mK). Accordingly, we propose using sample thicknesses verifying $L/\sqrt{D_s} \approx 0.5\,s^{0.5}$, i.e. $t_l \approx 0.1$ s. In this way, the temperature level just after the elbow, where the sensitivities to D_s and e_s are the largest, is high enough to provide a good signal-to-noise ratio.

On the other hand, figure 3(b) shows that $Sy(e_s)$ is always positive, since increasing the thermal effusivity of the sample leads to a temperature rise, as can be seen in figure 2. Moreover, $Sy(e_s)$ reaches an asymptotic value $Sy(e_s) = 1.0$ for all materials. However, this value is reached at different times depending on the thermal effusivity of the sample. In particular, for samples with a very high effusivity the highest $Sy(e_s)$ is obtained only at very long times. This result is related to the fact that the slope of $T_s(0)$ changes slowly for high thermal effusivity materials, while this change is abrupt for low effusors.

The effects of the finite duration of the laser pulse and heat losses are illustrated in figure 4. Simulations have been performed for a sample with $D_s = 4\,mm^2\,s^{-1}$ and $L = 1$ mm, with normalized energy for the laser pulse ($Q_\alpha\chi/e_s = 1$). The finite duration of the laser pulse appears at very short times, breaking the characteristic straight line with slope −0.5 corresponding to an ideal Dirac pulse. Simulations have been performed for the temporal shape of our pulsed laser, as given in section 2 ($\alpha = 1.46$ and $\tau = 0.132$ ms). By contrast, the effect of heat losses appears at long times after the laser pulse. For air backing, the temperature behaviour deviates from the horizontal straight line predicted for adiabatic conditions.

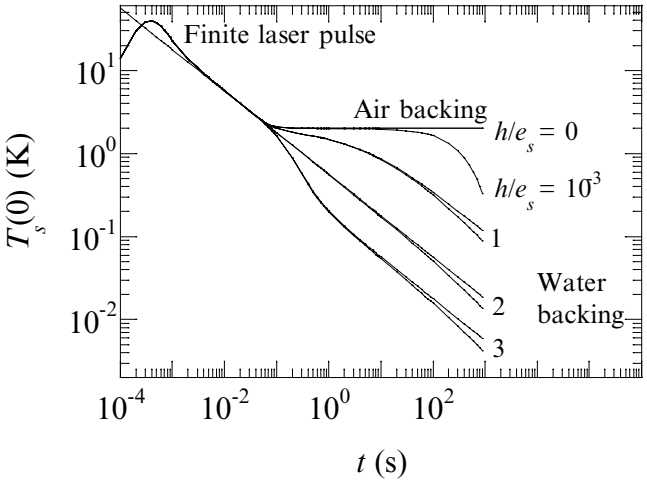

Figure 4. Effect of the finite duration of the laser pulse and heat losses. Simulations have been performed for $D_s = 4\,mm^2\,s^{-1}$ and $L = 1$ mm, with normalized energy for the laser pulse ($Q_\alpha\chi/e_s = 1$). The effect of the finite duration of the laser pulse has been simulated for the temporal shape of our pulsed laser ($\alpha = 1.46$ and $\tau = 0.132$ ms). For air backing, the effect of heat losses has been calculated for $h/e_s = 0$ and $10^{-3}\,s^{-0.5}$. For water backing, simulations have been performed for three sample thermal effusivities: (1) $e_s = 10^4\,W\,s^{0.5}\,m^{-2}\,K^{-1}$, (2) $e_s = 1580\,W\,s^{0.5}\,m^{-2}\,K^{-1}$ and (3) $e_s = 500\,W\,s^{0.5}\,m^{-2}\,K^{-1}$. For each of them results with $h = 0$ (upper curve) and $h = 10\,W\,m^{-2}\,K^{-1}$ (lower curve) are shown.

In a similar way, for water backing the temperature behaviour deviates from the straight line with slope −0.5. Simulations have been performed keeping the sample diffusivity and thickness constant, but changing its thermal effusivity: (1) $e_s = 10^4\,W\,s^{0.5}\,m^{-2}\,K^{-1}$, (2) $e_s = 1580\,W\,s^{0.5}\,m^{-2}\,K^{-1}$ and (3) $e_s = 500\,W\,s^{0.5}\,m^{-2}\,K^{-1}$. Results for $h = 0$ (adiabatic conditions) and $h = 10\,W\,m^{-2}\,K^{-1}$ are shown in figure 4. As can be seen, heat losses have a smaller effect when using water than when using air. The reason is twofold: on the one hand, with air backing there are heat losses at both sides of the samples,

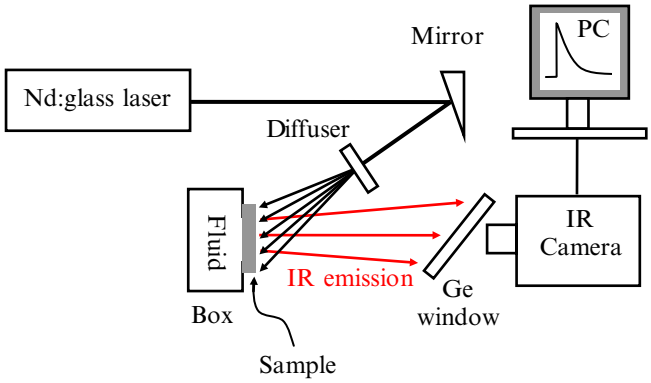

Figure 5. Diagram of the experimental setup.

while with a liquid backing heat losses appear only at the front surface; on the other hand, the temperature is lower for a liquid backing than for air, and therefore the heat flux is also lower since it is proportional to the temperature, as can be seen in equation (4*a*). According to the results shown in figure 4, both the finite duration of the heating pulse as well as heat losses must be included in the fitting of the experimental results to obtain accurate values of D_s and e_s.

4. Experimental results and discussion

In order to validate the method proposed in this manuscript to measure D_s and e_s simultaneously, we have performed measurements on reference solid samples covering a wide range of thermal transport properties: metals, alloys, vitreous carbon, ceramics and polymers.

The diagram of the experimental setup is shown in figure 5. A pulsed Nd : glass laser (1053 nm) with 'flat-top' spatial profile and adjustable energy (up to 25 J per pulse) is used as the heating source. The beam is directed onto the sample surface via a gold-coated mirror. In order to guarantee a uniform heating of the sample a holographic diffuser is placed 20 cm away from the sample surface. Sample sizes are 5 cm side squares in order to achieve 1D heat propagation. The sample is attached to the 4 cm × 4 cm window of a metallic box that can be filled with any non-reactive liquid. A poor thermal conducting paste is used to stick the sample edges to the box in order to reduce heat leaks during measurements. The IR radiation emitted by the sample is recorded by an IR camera (FLIR SC7500 working between 3 and 5 μm) provided with a 50 mm focal length lens. At its minimum working distance (about 35 cm) each pixel measures the average IR emission from a 140 mm-side square over the sample surface. Only the pixels placed on a 1 cm-side square at the centre of the sample are taken into consideration in order to reduce the influence of heat leaks from the sample to the box. A Ge window is used to protect the camera lens. We record images at frame rates in the range 1–3.5 kHz. Most samples are covered by a thin graphite layer (about 3 μm thick) in order to improve both the laser energy absorption and the sample IR emissivity. It is worth mentioning that the temperature rise above the ambient detected by the IR camera (ΔT) is not the actual surface temperature rise of the sample (its emissivity is not known), but it is proportional to $T_s(0)$.

The noise-equivalent temperature difference (NETD) of our IR camera is about 20 mK [15]. This value is obtained for a single pixel working with an integration time of 1.6 ms at 25 °C. However, we measure the average temperature over a large number of pixels (around 5000 pixels), thus reducing the noise level of the experiments down to 3–5 mK. Note that using an IR camera is not mandatory for this kind of measurement. A monolithic IR detector with a large active area (1–2 mm^2) connected to an oscilloscope is much cheaper but accurate enough.

Ten samples with known thermal properties were measured to assess the validity of the flash method to retrieve D_s and e_s simultaneously. Samples thicknesses were selected in order to verify $t_l = L^2/(\pi D_s) \approx 0.1$. This particular instant gives the position of the elbow, where the initial straight line with −0.5 slope is modified by the presence of the rear surface of the sample. In this way, we have a long enough time range (up to 6 s in our setup) to obtain the thermal effusivity of the sample before lateral heat flow invalidate the 1D model assumed in the theory. Figure 6 shows the results for two metallic and two polymeric samples: nickel, AISI-304 stainless steel, polycarbonate (PC) and polyether-ether-ketone (PEEK). Polymeric samples were studied with three backings: air, water and ethanol, while for the other samples only air and water backings were used. Experimental results are represented by dots and their corresponding curve fittings by continuous lines. For the sake of clarity temperature data for Ni and PC are shifted downwards. A least-squares fitting procedure has been implemented using the well-known Levenberg–Marquardt algorithm [16, 17], and the fittings have been done with respect to the inverse Laplace transform of equation (5). Four free parameters have been used in the fittings: $Q_o\chi/e_s$, h/e_s, $L/\sqrt{D_s}$ and e_f/e_s. To better evaluate the quality of the fittings, the residuals, i.e. the normalized difference between experimental data and fitted values, $(T_s(0)_{exp} - T_s(0)_{fit})/T_s(0)_{exp} \times 100$, are also plotted. They are lower than 2% in the whole time range. The retrieved diffusivity and effusivity data for the ten samples are summarized in table 1, where the materials are listed according to decreasing values of the thermal effusivity. Each value is the average of three consecutive measurements.

As can be observed in table 1, thermal diffusivity values for all the samples agree with the literature values in both configurations: using air or water as backing fluid. As the thermal effusivity of polymers is very close to that of ethanol ($e_{ethanol} = 560\,W\,s^{0.5}\,m^{-2}\,K^{-1}$), no thermal diffusivity can be obtained for these materials using ethanol as backing fluid (since there is no noticeable change in the −0.5 slope) in agreement with the theoretical prediction.

Regarding the thermal effusivity, which is the main goal of this work, it is retrieved accurately provided $e_s \leqslant 3e_f$, as is the case for polymers, Sigradur G glassy carbon and bismuth, when measured with water backing. For samples verifying $e_s >> 3e_f$, as is the case of copper, zinc, nickel, lead, alumina and AISI-304, the thermal effusivity is underestimated and this error is more pronounced as the thermal effusivity of the sample differs from that of the water. The origin of this drawback arises from the fact that for good thermal effusors, the sensitivity of $T_s(0)$ to effusivity is low close to the elbow

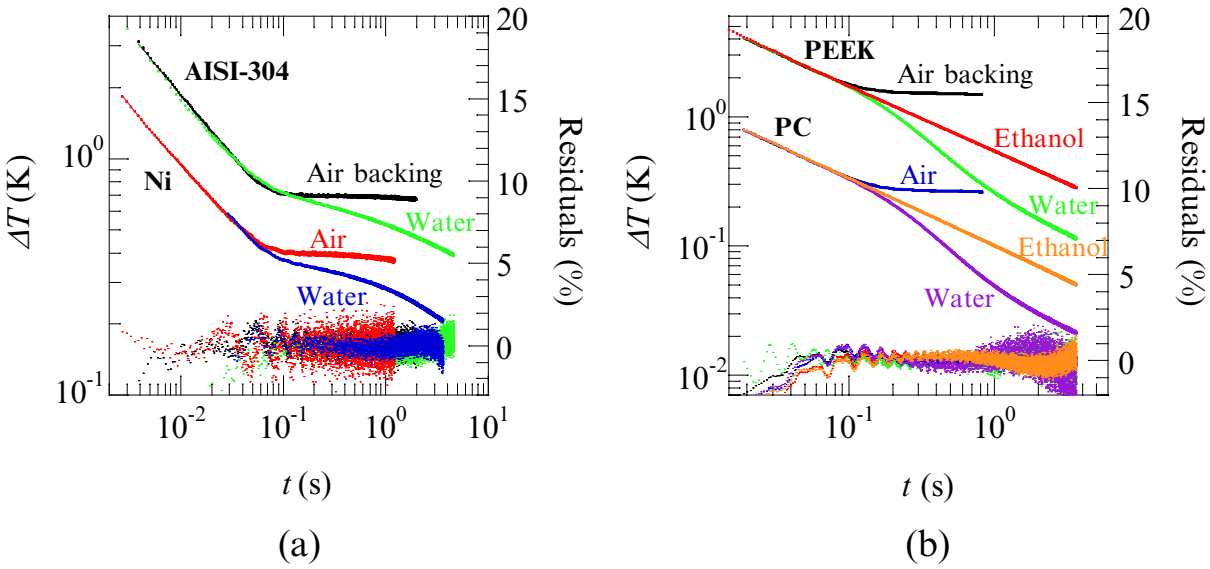

Figure 6. Temperature rise above ambient as a function of time after the heating pulse for different materials. Dots are the experimental data and continuous lines the fitting to the theory. Temperature data for Ni and PC are shifted. (a) Metallic samples. (b) Polymers. Polymeric samples were studied with three backings: air, water and ethanol, whereas metallic samples were studied only with air and water backings. Residuals are also plotted to visualize the quality of the fits.

Table 1. Thermal diffusivity (D_s) and effusivity (e_s) of the materials studied in this work. The uncertainty is discussed in the text.

Material	L (mm)	D_s air backing ($mm^2 s^{-1}$)	D_s water backing ($mm^2 s^{-1}$)	D_s literature[a] ($mm^2 s^{-1}$)	e_s water backing ($W s^{0.5} m^{-2} K^{-1}$)	e_s literature[a] ($W s^{0.5} m^{-2} K^{-1}$)
Cu	3.248	107	120	117	9100	37 140
Ni	2.065	21	21	23.0	12 000	18 910
Zn	3.116	42	44	41.8	9800	17 942
Alumina	1.035	8.4	8.6	7.6–10.3	8600	9430–10 900
AISI-304	0.897	3.8	4.1	3.95	6800	7498
Pb	2.176	23	24	24.1	6800	7190
Bi	1.040	6.0	6.1	6.55	3000	3050
Glassy carbon	1.088	6.6	6.6	6.2	2300	2530
PEEK	0.259	0.17	0.18	0.145	640	655
PC	0.261	0.14	0.15	0.13–0.15	550	523–563

[a] [11, 18,19].

and it slowly increases with time. In fact, very long times must be reached in order to obtain a significant sensitivity to effusivity, as can be seen in figure 3(b). However, those data corresponding to such long times are affected by lateral heat flux and therefore cannot be used in the fitting to equation (5), which assumes 1D heat propagation.

The two polymers studied in this work were also analysed using ethanol as backing fluid. The obtained effusivity values are: $e_{PC} = 550 W s^{0.5} m^{-2} K^{-1}$ and $e_{PEEK} = 640 W s^{0.5} m^{-2} K^{-1}$. Note that they agree with the values obtained with water backing and with the literature values.

The uncertainty in D_s in flash measurements with air backing is in the range 3–5%, as was shown in a previous work [12]. The uncertainty in D_s with water backing depends on the effusivity of the sample, as discussed in section 3. It is small (3–5%) for samples verifying $e_s >> e_w$ or $e_s << e_w$ but it increases as the effusivity approaches that of water. In the limit, for samples with effusivity close to that of the water, D_s cannot be obtained since its sensitivity is close to zero (see figure 3(a)). In these cases, the practical solution is replacing water by another fluid with different effusivity, e.g. ethanol. On the other hand, as discussed above, only thermal effusivities satisfying $e_s \leqslant 3e_f$ can be measured. The uncertainty is around 5–10%. Accordingly, the experimental results are given with two significant figures (see table 1).

Notice that only room temperature (RT) measurements have been performed. In any event, there are several liquids with boiling points in the range 200–300 °C (such as glycerine, 290 °C) that could be used to measure D_s and e_s above RT. It is worth mentioning that the eutectic liquid alloy made of Ga, In and Sn has a boiling point higher than 1300 °C. Owing to its low toxicity and wetting ability [20], introducing this liquid metal paves the way to use the method proposed in this work at high temperatures. In this case heat transfer by convection to the backing fluid cannot be neglected. This issue can be overcome by placing both the sample and the backing fluid in a horizontal position. Otherwise this heat transfer by convection should be included in the theoretical model.

5. Conclusions

In this work, we have addressed the challenging task of measuring the thermal effusivity of solids in a fast and accurate manner. We have improved the flash method in the front configuration to deal with a two-layer system made of the plate under study and a reference liquid. It is shown that the time evolution of the surface temperature of the solid plate is sensitive to thermal diffusivity and to the thermal mismatch between solid and liquid, which depends on their ratio of thermal effusivities. IR thermography measurements performed on ten samples covering a wide range of thermal effusivities confirm that the thermal effusivity can be retrieved accurately, provided the thermal effusivity of the sample is not higher than three times the thermal effusivity of the reference liquid. Since water is the most accessible liquid with high thermal effusivity, the highest effusivity that can be measured with this technique is about $5000\,\mathrm{W\,s^{0.5}\,m^{-2}\,K^{-1}}$. Although good effusors are out the application range of this technique, the transport properties of many materials of industrial interest such as polymers, composites, ceramics, inorganic oxides, etc can be retrieved.

Acknowledgments

This work has been supported by the Ministerio de Ciencia e Innovación (MAT2011-23811), by Gobierno Vasco (IT619-13), by UPV/EHU (UFI 11/55), by CINVESTAV Unidad Mérida and by CONACYT beca mixta.

References

[1] Salazar A 2003 On thermal diffusivity *Eur. J. Phys.* **24** 351–8
[2] Marin E 2007 The role of thermal properties in periodic time-varying phenomena *Eur. J. Phys.* **28** 429–45
[3] Parker W J, Jenkins R J, Butler C P and Abbott G L 1961 Flash method of determining thermal diffusivity, heat capacity and thermal conductivity *J. Appl. Phys.* **32** 1679–84
[4] Balageas D L 1989 Thermal diffusivity measurement by pulsed methods *High Temp. High Press.* **21** 85–96
[5] Carslaw H S and Jaeger J C 1959 *Conduction of Heat in Solids* (Oxford: Oxford University Press) p 361
[6] Murabayashi M, Takahashi Y and Mukaibo T 1970 Measurement of heat capacity at high temperatures by laser flash method *J. Nucl. Sci. Technol.* **7** 312–16
[7] Takahashi Y, Yokohama H, Kadokura H, Sekine Y and Mukaibo T 1979 Laser-flash calorimetry: I. Calibration and test on alumina heat-capacity *J. Chem. Thermodyn.* **11** 379–94
[8] Shinzato K and Baba T 2001 A laser flash apparatus for thermal diffusivity and specific heat capacity measurements *J. Therm. Anal. Calorim.* **64** 413–22
[9] Kim S K and Kim Y J 2007 Improvement of specific heat measurement by the flash method *Thermochim. Acta* **455** 30–3
[10] Depriester M, Hus P, Delenclos S and Hadj Sahraoui A 2005 New methodology for thermal parameter measurements in solids using photothermal radiometry *Rev. Sci. Instrum.* **76** 074902
[11] Vales-Pinzon C, Ordonez-Miranda J and Alvarado-Gil J J 2012 Photothermal characterization of the thermal properties of materials using four characteristic modulation frequencies in two-layer systems *J. Appl. Phys.* **112** 064909
[12] Pech-May N W, Mendioroz A and Salazar A 2014 Generalizing the flash technique in the front-face configuration to measure the thermal diffusivity of semitransparent solids *Rev. Sci. Instrum.* **85** 104902
[13] Stehfest H 1970 Algorithm 368: numerical inversion of Laplace transforms *Commun. ACM* **13** 47–9
[14] Stehfest H 1970 Remark on algorithm 368: numerical inversion of Laplace transforms *Commun. ACM* **13** 624
[15] Maldague X P V 2001 *Theory and Practice of Infrared Technology for Nondestructive Testing* (New York: Wiley) p 101
[16] Levenberg K 1944 A method for the solution of certain non-linear problems in least squares *Quart. Appl. Math.* **2** 164–8
[17] Marquardt D W 1963 An algorithm for least-squares estimation of nonlinear parameters *SIAM J. Appl. Math.* **11** 431–41
[18] Touloukian L R, Powell R W, Ho C Y and Nicolasu M C 1973 *Thermal Diffusivity* (New York: IFI/Plenum)
[19] Çengel Y A 2003 *Heat Transfer: a practical Approach* (Boston, MA: McGraw-Hill)
[20] Plevachuk Y, Sklyarchuk V, Eckert S, Gerbeth G and Novakovic R 2014 Thermophysical properties of the liquid Ga–In–Sn eutectic alloy *J. Chem. Eng. Data* **59** 757–63